Local human movement patterns and land use impact exposure to zoonotic malaria in Malaysian Borneo

Kimberly M Fornace*[1], Neal Alexander[2], Tommy R Abidin[3], Paddy M Brock[4], Tock H Chua[3], Indra Vythilingam[5], Heather M. Ferguson[4], Benny O. Manin[3], Meng L. Wong[5], Sui Hann Ng[3], Jon Cox[1], Chris J Drakeley[1]

1. Faculty of Infectious and Tropical Diseases, London School of Hygiene and Tropical Medicine, London, UK
2. Department of Infectious Disease Epidemiology, London School of Hygiene and Tropical Medicine, London, UK
3. Department of Pathobiology and Medical Diagnostics, Faculty of Medicine and Health Sciences, Universiti Malaysia Sabah, Kota Kinabalu, Malaysia
4. Institute of Biodiversity, Animal Health and Comparative Medicine, College of Medical, Veterinary and Life Sciences, University of Glasgow, UK
5. Parasitology Department, Faculty of Medicine, University of Malaya, Kuala Lumpur, Malaysia

*** Corresponding author:**

Kimberly M Fornace

Kimberly.Fornace@lshtm.ac.uk

London School of Hygiene and Tropical Medicine, Keppel Street, London, WC1E 7HT, UK

+44 (0) 20 7927 2010

Abstract: (150 max)

Human movement into insect vector and wildlife reservoir habitats determines zoonotic disease risks; however, few data are available to quantify the impact of land use on pathogen transmission. Here, we utilise GPS tracking devices and novel applications of ecological methods to develop fine-scale models of human space use relative to land cover to assess exposure to the zoonotic malaria *Plasmodium knowlesi* in Malaysian Borneo. Combining data with spatially explicit models of mosquito biting rates, we demonstrate the role of individual heterogeneities in local space use in disease exposure. At a community level, our data indicate that areas close to both secondary forest and houses have the highest probability of human *P. knowlesi* exposure, providing quantitative evidence for the importance of ecotones. Despite higher biting rates in forests, incorporating human movement space use into exposure estimates illustrates the importance of intensified interactions between pathogens, insect vectors and people around habitat edges.

Keywords (min 3):

Disease ecology, spatial epidemiology, *Plasmodium knowlesi*, malaria, human movement, land use

45 **Introduction:**

46

47 Environmental change and human encroachment into wildlife habitats are key drivers in the
48 emergence and transmission of zoonotic diseases (1, 2). Individual movements into different
49 habitats influence exposure to disease vectors and animal reservoirs, determining risk and
50 propagation of vector-borne diseases (3-5). Increased contact between these populations is
51 theorised to drive increases of the zoonotic malaria *Plasmodium knowlesi* in Malaysian Borneo, now
52 the main cause of human malaria within this region. *P. knowlesi* is carried by long- and pig-tailed
53 macaques (*Macaca fascicularis* and *M. nemestrina*) and transmitted by the *Anopheles leucospryphus*
54 mosquito group, both populations highly sensitive to land cover and land use change (6). Although
55 higher spatial overlap between people, macaques and mosquito vectors likely drives transmission,
56 the impact of human movement and land use in determining individual infection risks is poorly
57 understood (7).

58

59 The emergence of the zoonotic malaria *Plasmodium knowlesi* has been positively associated with
60 both forest cover and historical deforestation (8, 9). However, out of necessity, statistical
61 approaches to assess environmental risk factors for *P. knowlesi* and other infectious diseases
62 typically evaluate relationships between disease metrics and local land cover surrounding houses or
63 villages. While an individual may spend most of their time within the vicinity of their residence, this
64 area does not necessarily represent where they are most likely to be exposed to a disease. This is
65 supported by varying associations between *P. knowlesi* occurrence and landscape variables at
66 different distances from households, ranging from 100m to 5km, likely partially due to human
67 movement into different surrounding habitats (8, 10). Although land cover variables describing
68 physical terrestrial surfaces are frequently incorporated into disease models, land use is rarely
69 quantified. Land use is commonly defined as "the arrangements, activities, and inputs that people
70 undertake in certain land cover types" (11). Places with the similar types of land cover may be used

very differently, with the activities and frequencies with which people visit these places determining the spatial distribution of disease (1).

Mathematical modelling studies have revealed the importance of spatial variation in contact rates due to the movement of individuals through heterogeneous environments with varying transmission intensity (12). A multi-species transmission model of *P. knowlesi* highlighted the role of mixing patterns between populations in different ecological settings in determining the basic reproductive rate and subsequent modelling studies illustrate the sensitivity of this disease system to population densities of both people and wildlife hosts (7, 13). However, although mechanistic models have been extended to explore the potential importance of these heterogeneities in disease dynamics, there are inherent constraints on model complexity and most models make simplistic assumptions about the habitat uses of different populations.

Empirical data on human population movement is increasingly available, allowing assessment of the impact of mobility on infectious disease dispersion and risks (5). On larger spatial scales, mobile phone data has revealed the role of human migration in the transmission of infectious diseases such as malaria, dengue and rubella (14-16).Although this data can provide insights into long range movements, spatial resolution of this data is limited, particularly in areas with poor or no mobile coverage, such as forested areas (17). Alternatively, the advent of low-cost GPS tracking devices allows quantification of fine-scale movements, demonstrating marked heterogeneity in individual movement and risk behaviours (3, 18). Combining these data with detailed data on land cover and vector dynamics can provide new insights into how landscapes affect *P. knowlesi* transmission.

Previous studies of *P. knowlesi* have relied on questionnaire surveys, identifying self-reported travel to nearby plantations and forest areas as a risk factor for *P. knowlesi* and other malaria infections (e.g. (19-21)). However, the resultant spatial range and frequency of these movements remain

97 unknown and the definition of different habitat types is entirely subjective. Further, little is known
98 about differences in local movement patterns in different demographic groups. While infections in
99 male adults have been linked to forest and plantation work, it is unknown whether infections
100 reported in women and young children are likely to arise from exposure to similar environments
101 (22). The main mosquito vector in this area, *An. balabacensis*, is primarily exophagic and has been
102 identified in farm, forest and village areas near houses (23, 24). Macaque populations are reported
103 in close proximity to human settlements and molecular and modelling studies suggest transmission
104 remains primarily zoonotic in this area (7, 25, 26). A case control study detected higher abundances
105 of *An. balabacensis* near *P. knowlesi* case housesholds, suggesting the possibility of peri-domestic
106 transmission (24). Understanding the importance of these habitats is essential to effectively target
107 intervention strategies and predict impacts of future environmental changes.
108
109 Key questions remain about where individuals are likely to be exposed to *P. knowlesi* and how
110 landscape determines risk. Functional ecology approaches allow the distribution of different
111 populations to be modelled based on biological resources and relate transmission to landscape and
112 environmental factors (27). Within wildlife ecology, numerous methods have been developed to
113 estimate utilisation distributions (UDs), the probability of an individual or species being within a
114 specific location during the sampling period (28). Although these methods traditionally rely on kernel
115 density smoothing, kernel density estimates may not actually reflect time individuals spend in a
116 specific location if there is substantial missing data or irregular time intervals. Alternatively, biased
117 random bridges (BRBs) improve on these methods by estimating the UD as a time-ordered series of
118 points, taking advantage of the autocorrelated nature of GPS tracks to bias movement predictions
119 towards subsequent locations in a time series (29). This allows for interpolation of missing values
120 and adjustment for spatial error to estimate UDs representing both the intensity (mean residence
121 time per visit) and frequency of individual visits to specific locations. By integrating these estimates
122 of individual space use with detailed spatial and environmental data in a Bayesian framework, fine-

scale patterns of human land use can be predicted and overlaid with spatiotemporal models of mosquito distribution. This allows exploration how landscape composition, as well as configuration and connectivity between habitats, impacts human exposure to *P. knowlesi* and other vector-borne and zoonotic diseases.

Focusing on one aspect of land use, human movement and time spent within different land cover types, we explored the role of heterogeneity in local space use on disease exposure. Rolling cross-sectional GPS tracking surveys were conducted in two study areas with on-going *P. knowlesi* transmission in Northern Sabah, Malaysia (Matunggong and Limbuak (30)). We aimed to characterise local movement patterns and identify individuals and locations associated with increased *P. knowlesi* exposure risks by: 1. analysing individual movement patterns and developing predictive maps of human space use relative to spatial and environmental factors, 2. modelling biting rates of the main vector *An. balabacensis*, and 3. assessing exposure risks for *P. knowlesi* based on predicted mosquito and human densities (Figure 1) Integrating these three approaches allowed a uniquely spatially explicit examination of disease risk.

Figure 1. Analysis methods used to estimate individual and community-level exposure to *P. knowlesi* sporozoite positive *An. balabacencis* bites

Methods

Study site

This study was conducted in two rural communities in Northern Sabah, Malaysia: Matunggong, Kudat (6°47N, 116°48E, population: 1260) and Limbuak, Pulau Banggi (7°09N, 117°05E, population: 1009) (Figure 2). These areas were the focus for integrated entomology, primatology and social science studies for risk factors for *P. knowlesi* (https://www.lshtm.ac.uk/research/centres-projects-

149 groups/monkeybar), with clinical cases and submicroscopic infections reported from both sites and
150 *P. knowlesi* sero-prevalence estimated as 6.8% and 11.7% in Matunggong and Limbuak respectively
151 (30).
152
153 Demographic data and GPS locations of primary residences were collected for all individuals residing
154 in these areas (30). Potential spatial and environmental covariates for these sites were assembled
155 from ground-based and remote-sensing data sources (Supplementary Table 1). The enhanced
156 vegetation index (EVI) was used to capture temporal changes in vegetation levels; this index
157 captures photosynthetic activity and has higher sensitivity in high biomass areas compared to the
158 normalised difference vegetation index (NDVI) frequently used. Due to the high cloud cover within
159 this area, EVI at a high spatial resolution could not be obtained for all time periods. Instead, EVI data
160 at a lower spatial but higher temporal resolution was used and monthly averages were calculated
161 from all available cloud-free data and resampled to 30m per pixel (31).
162
163 **Figure 2.** A. Location of study sites and tracked houses (households with one or more individual GPS
164 tracked) and survey houses (households with only questionnaire data collected and used for
165 prediction) in B. Matunggong, Kudat and C. Limbuak, Banggi; description of land cover classification
166 and survey methodology in (30)
167
168 *GPS tracking survey*
169 A minimum of 50 participants per site were targeted in a rolling cross-sectional survey (32). During
170 pre-defined two-week intervals, randomly selected participants from comprehensive lists of eligible
171 community members were asked to carry a QStarz BT-QT13000XT GPS tracking device (QStarz,
172 Taipei, Taiwan) programmed to record coordinates continuously at one-minute intervals for at least
173 14 days regardless of individual movement. Individuals were excluded if they were not primarily
174 residing in the study area, under 8 years old or did not consent. Trained fieldworkers visited the

175 participant every two days to confirm the device was functioning, replace batteries and administer
176 questionnaires on locations visited and GPS use. Fieldworkers recorded whether the device was
177 working and if the individual was observed carrying the GPS device to assess compliance. Individuals
178 were excluded from analysis if insufficient GPS data were collected (less than 33% of sampling
179 period) or individuals were observed not using the device for two or more visits.
180
181 *Human space use*
182 Biased random bridges (BRBs) were used to calculate individual utilisation distributions (UDs), the
183 probability of an individual being in a location in space within the sampled time period (29). Within
184 this study, large proportions of GPS fixes were missed due to technical issues with batteries and GPS
185 tracking; BRBs were used to interpolate between known locations and adjust for missing data, using
186 the time series GPS data to provide a more accurate estimate of space use. UDs were calculated
187 separately for each individual for all movement and night-time only movements (6pm – 6am).
188
189 To fit BRBs, we estimated the maximum threshold between points before they were considered
190 uncorrelated (T_{max}) as 3 hours based on typical reported activity times. The minimum distance
191 between relocations (L_{min}), the distance below which an individual is considered stationary, was set
192 at 10m to account for GPS recording error based on static tests. Finally, the minimum smoothing
193 parameter (h_{min}), the minimum standard deviation in relocation uncertainty, was set as 30m to
194 account for the resolution of habitat data and capture the range of locations an individual could
195 occupy while being recorded at the same place (28, 29). Estimates of the core utilisation area (home
196 range) were based on the 99th percentile, representing the area with a 99% cumulative probability
197 distribution of use by the sampled individual.
198
199 To assess relationships between space use and environmental factors and develop predictive maps
200 of community space use, we fit resource utilisation functions, regression models in which the UDs

are used as the response variable, improving on models using raw GPS count points as the response when there is location uncertainty and missing data (33). The probability density function (UD) per individual was rasterised to 30m^2 grid cells and environmental and spatial covariates extracted for each grid cell. Potential environmental covariates included distance to the individual's own house, distance to closest house, distance to roads, land use class (forest, agriculture, cleared or water), distance to forest edge, elevation and slope (Supplementary table 1). Resource utilisation was modelled as a Bayesian semi-continuous (hurdle) model with two functionally independent components, a Bernoulli distribution for probability of individual *i* visiting a specific grid cell *j* (ω_{ij}) and a gamma distribution for the UD in grid cells visited (y_{ij}) (34, 35). For each individual, we defined absences to be all grid cells with a UD less than 0.00001, indicating a very low probability the individual visited this grid cell during the study period. We included all presences (grid cells with a UD > 0.00001) and randomly subsampled equal numbers of absences (grid cells not visited) for each individual as including equal numbers of presences and absences can improve predictive abilities of species distribution models (36). The utilisation distribution for grid cells visited is defined as:

$$y_{ij} = \begin{Bmatrix} \text{Gamma}\left(\frac{\mu_{ij}^2}{\sigma^2}, \frac{\sigma^2}{\mu_{ij}}\right) \text{with probability } 1 - \phi_{ij} \\ 0 \text{ with probability } \phi_{ij} \end{Bmatrix}$$

Where the mean of y_{ij} is given by:

$$\mu_{ij} = \mathrm{E}\left(y_{ij} | X_{ij}^T\right) = \left(1 - \omega_{ij}\right) v_{ij}$$

The full model was specified as:

$$\omega_{ij} \sim \text{Bernoulli}\left(\phi_{ij}\right)$$

With the linear predictor for the Bernoulli model specified as:

$$\text{logit}\left(\phi_{ij}\right) = \beta_0 + X_{ij}^T \beta_i + \gamma_j$$

222

223 Where β_0 represents the intercept, $X_{ij}^T\beta_i$ represents a vector of covariate effects and γ_j represents

224 the additive terms of random effects for individual. For the Gamma component, σ^2 is the variance

225 and the linear predictor υ_{ij} is specified as:

226

$$\log(\upsilon_{ij}) = \alpha_0 + X_{ij}^T\alpha_i + \varphi_j$$

227

228 With α_0 representing the intercept, $X_{ij}^T\alpha_i$ representing a vector of coordinates and φ_j representing

229 the random effects. Weakly informative normal priors specified as Normal (0,1/0.01) were used for

230 all intercepts and coefficients. Bayesian inference was implemented using integrated nested Laplace

231 approximation (INLA) (37). This approach uses a deterministic algorithm for Bayesian inference,

232 increasing computational efficiency relative to Markov chain Monte Carlo and other simulation-

233 based approaches (34). We did not explicitly include spatial autocorrelation as several distance-

234 based covariates were included (e.g. distance from own house) (33). Predictive models used data for

235 all individuals aged 8 or over residing in these communities (Table 1) and models were limited to

236 land areas within 5km of households included in the study site. Separate models were fit for each

237 site.

238

239 *Exposure to infected vectors*

240

241 To estimate vector biting rates, we assembled data from 328 nights of human landing catches (HLCs)

242 conducted with 5km of the Matunggong study site while GPS tracking was on-going, including:

243 monthly longitudinal surveillance (23), investigations surrounding households of cases and controls

244 (24), and environmentally stratified outdoor catches (38) (Supplementary table 2). We limited this

245 data to counts of *An. balabacensis*, the primary *knowlesi* vector which comprises over 95% of

246 *Anopheles* caught in this region. As one experiment only collected mosquitoes for 6 hours, we fit a

linear model of all available data vs totals after 6 hour catches to estimate the total numbers of *An. balabacensis* which would have been caught over 12 hours for these data (R^2= 0.85). Plausible environmental covariates were assembled, including land use type, slope, aspect, elevation, topographic wetness index, EVI, population density and average monthly temperature and rainfall. To select variables for inclusion, Pearson correlation analysis was used to assess multicollinearity between selected environmental variables. As topographic slope and TWI had a strong negative correlation, only TWI was included in the analysis. The autocorrelation function (ACF) and partial autocorrelation function (PACF) were used to explore correlation between time lags.

A Bayesian hierarchical spatiotemporal model was implemented using counts of *An. balabacensis* bites as the outcome, denoted as m_{it}; j = 1…n; t = 1…n; where j indexes location and t indexes month. The log number of person-nights per catch was included as an offset to adjust for numbers of catchers conducting HLCs during different experiments. As the data were over dispersed, a negative binomial distribution was used to model m_{it}. The linear predictor was specified as:

$$\log(\mu_{jt}) = \log(N_{jt}) + Z_0 + D_{jt}^T Z + w_j + e_t$$

Where N_{ijt} represents the number of person-nights for each HLC catch, Z_0 represents the intercept, $D_{jt}^T Z$ represents a vector of covariates, w_j is the spatial effect and e_t is the temporal effect. The temporal effect e_t was included as a fixed effect, random effect or temporally structured random walk model of order 1 in candidate models (39). The spatial effect w_j was modelled as a Matern covariance function between locations s_j and s_k:

$$W \sim Multivariate\ Normal\ (0, \Sigma)$$

$$\Sigma_{hk} = Cov(\xi(s_h), \xi(s_k)) = Cov(\xi_h, \xi_k) = \frac{\sigma^2}{\Gamma(\lambda) 2^{\lambda-1}} (\kappa||s_h - s_k||)^{\lambda} K_{\lambda}(\kappa||s_h - s_k||)$$

Where $||s_h - s_k||$ denotes the Euclidean distance between locations s_h and s_k, $\xi(s)$ is the latent Gaussian field accounting for spatial correlation, σ^2 is the spatial process variance and K_λ is a modified Bessel function of the second kind and order $\lambda > 0$. κ is a scaling parameter related to r, the distance at which spatial correlation becomes negligible, by $r = \sqrt{8\lambda}/\kappa$. A stochastic partial differential equations (SPDE) approach was used, representing the spatial process by Gaussian Markov random fields (GMRF) by partitioning the study area into non-intersecting triangles (40). This approach represents the covariance matrix Σ by the inverse of the precision matrix Q of the GMRF (34, 40). Prior distributions were specified on fixed effects and hyperparameters. A vague normal prior distribution was used for the intercept. Weakly informative priors were used for fixed effects specified as $N(1,1/0.01)$. Priors for spatial hyperparameters were specified as range $r \sim N(10, 1/0.01)$ and standard deviation $\sigma \sim N(0.1, 1/0.01)$ as described by Lindgren and Rue (39).

As these vectors are rarely reported indoors (24) and HLCs were primarily conducted outside, we excluded areas within houses for calculations of exposure risks. The proportion of infectious mosquitoes, c, was parameterised using a beta distribution for *P. knowlesi* sporozoite rates within this site; with only 4 out of 1524 collected mosquitoes positive, it was not possible to look at variations of infection rates by time and space. Spatially explicit exposure risks were calculated as derived quantity from human resource utilisation, mosquito biting rate models and probability of *P. knowlesi* sporozoite positivity. Individual exposure risk was explored using a simple exposure assessment model where the number of infected bites received by an individual is the sum of bites by infected vector across all locations visited, with the number of infectious bites received by individual i in month t as:

$$r_{it} = c \sum_{j=1}^{J} y_{ij} m_{jt}$$

292 Where j indexes the grid cells visited, y_{ij} is the utilisation distribution, m_{jt} is the number of bites per
293 individual in that cell and month, and c is the proportion of infectious mosquitoes (4). To evaluate
294 places associated with exposure for the entire community, we calculated the number of infectious
295 bites per grid cell each month as:

$$r_{jt} = c \sum_{i=1}^{I} Y_{ij} m_{jt}$$

296 Where Y_{ij} is the predicted utilisation distribution for all individuals within the community per grid cell
297 j. All analyses were conducted in R version 3.5, with Bayesian models implemented using Integrated
298 Nested Laplace Approximation (INLA) (37). Model fit was assessed using deviance information
299 criteria (DIC) and area under the receiver operating curve (AUC), root mean square error (RMSE) or
300 conditional predictive ordinate (CPO) (41).
301
302 *Ethics approval*
303 This study was approved by the Medical Research Sub-Committee of the Malaysian Ministry of
304 Health and the Research Ethics Committee of the London School of Hygiene and Tropical Medicine.
305 Written informed consent was obtained from all participants or parents or guardians and assent
306 obtained from children under 18.
307
308 **Results:**
309
310 Between February 2014 and May 2016, 285 consenting people participated in the GPS tracking study
311 with 243 included in the final analysis including 109 in Limbuak and 134 in Matunggong (Table 1).
312 The most commonly reported occupation was farm or plantation work (n=73), primarily conducted
313 within the immediate vicinity of the house. A total of 3,424,913 GPS points were collected,
314 representing 6,319,885 person-minutes of sampling time. Median sampling duration was 16.27 days
315 (IQR 13.72 – 19.97), with points recorded for a median of 59.1% (IQR: 46.9% - 71.1%) of the sampling

duration. Maximum distances travelled ranged from no travel outside the house to 116km, with a median distance travelled of 1.8km. Utilisation distributions (UDs), the probability of an individual being in a location in space within a given time (Figure 3), varied by gender and occupation . Individuals at the more rural Limbuak site covered larger distances (Table 2), with the largest distances covered by individuals reporting primary occupations of fishing (n=5) and office work (n=9). Although substantial differences were reported in all movements (24 hour sampling) between seasons, no seasonal differences were observed in human movements during peak *Anopheles* biting times (6pm-6am).

Table 1. Baseline characteristics of study site communities and sampled populations

	Matunggong		Limbuak	
	Sampled	Community*	Sampled	Community*
N	134	958	109	633
Gender				
Male, % (n)	51.5% (69)	46.1% (442)	47.7% (52)	46.1% (292)
Women, % (n)	48.5% (65)	53.9% (516)	52.3% (57)	53.9% (341)
Age in years, median (IQR)	31 (17 – 53)	32.5 (8 – 51)	29 (15 – 46)	30 (15 – 47)
Main occupation, % (n)				
Farming	29.9% (40)	28.6% (274)	7.3% (8)	10.2% (65)
Plantation work	10.4% (14)	8.6% (82)	10.1% (11)	7.6% (48)
Student	26.1% (35)	27.7% (265)	26.6% (29)	21.0% (133)
Other	6.7% (9)	9.1% (87)	15.6% (17)	14.4% (91)
No employment/ housewife	26.9% (36)	26.1% (250)	40.4% (44)	46.8% (296)

* Community includes all individuals eligible for these surveys (residents ages 8 and over)

Figure 3. Human movement relative to habitat. A. Example of GPS tracks from a 22-year-old male plantation worker in Matunggong over aerial imagery, B. Individual utilisation distribution calculated from GPS tracks

Table 2. Home range estimates by demographic group and site

	Area of 99% UD for all movement (hectares) Median (IQR)	Area of 99% UD from 6pm – 6am (hectares) Median (IQR)
Demographic group		
Men	32.09 (7.07, 148.93)	4.50 (2.79, 19.53)
Women	74.25 (12.24, 320.74)	6.08 (2.79, 24.17)
Children (under 15)	26.01 (6.39, 151.94)	3.83 (2.79, 8.73)
Occupation		
Farming	29.34 (8.15, 324.38)	6.75 (2.79, 19.80)
Plantation work	49.14 (9.72, 201.33)	4.59 (2.79, 27.72)
Fishing	442.49 (40.07, 1189.00)	227.16 (4.05, 465.14)
Office work	96.80 (63.61, 256.75)	13.63 (2.88, 20.14)
Other	19.98 (6.30, 26.82)	2.97 (2.61, 18.27)
No employment/ housewife	43.38 (11.97, 157.59)	3.60 (2.79, 19.12)
Site		
Limbuak	99.99 (24.57, 387.54)	7.74 (2.88, 58.05)
Matunggong	12.02 (3.94, 85.55)	2.97 (2.70, 11.77)
Season		
Dry (February – July)	28.62 (5.45, 252.45)	4.19 (2.79, 19.60)
Wet (August – January)	54.90 (17.23, 160.99)	4.64 (2.79, 19.35)

For both study areas, we developed models of community space use during peak mosquito biting hours (6pm – 6am), in the form of resource utilisation functions, predictions of time- and space-specific UDs on the basis of spatial and environmental variables (28). Between 6pm – 6am, human space use (UDs) was mostly predictable and negatively correlated with distance from the individual's house, other houses, roads and slope. The AUC for presence/ absence models was 0.936 for Matunggong and 0.938 for Limbuak and RMSE for the overall model was 0.0073 and 0.0043 for Matunggong and Limbuak respectively. While individuals were more likely to use areas further away from forests in the Matunggong site, human space use was positively correlated with proximity to forests in the Limbuak site (Table 3). Despite marked differences between different demographic groups and seasons observed during 24 hour movements, these factors did not improve the predictive power of the model for movements between 6pm and 6am.

348 **Table 3.** Estimated coefficients for fixed effects of resource utilisation functions (6pm – 6am)

	Matunggong			Limbuak		
	Mean	SD	95% CI	Mean	SD	95%CI
Probability of presence/ absence						
Intercept	3.383	0.839	3.218, 3.547	3.571	0.104	3.368, 3.775
Distance from own house (km)	-0.954	0.006	-0.966, -0.942	-0.543	0.003	-0.548, -0.539
Distance from forest (km)	5.997	0.177	-5.650, 6.344	-1.845	0.050	-1.944, -1.746
Distance from road (km)	-5.552	0.057	-5.663, -5.441	-3.656	0.019	-3.694, -3.618
Distance from houses (km)	-0.504	0.030	-0.563, -0.444	0.176	0.007	0.162, 0.189
Elevation (100 MSL)	-0.710	0.025	-0.759, -0.662	-1.268	0.037	-1.340, -1.197
Slope (degrees)	-0.0244	0.002	-0.028, -0.021	-0.009	0.001	-0.012, -0.006
Utilisation distributions for locations present						
Intercept	-6.846	0.866	-8.549, -5.147	-5.676	1.017	-7.673, -3.681
Distance from own house (km)	-0.583	0.004	-0.590, -0.576	-0.308	0.002	-0.311, -0.305
Distance from forest (km)	12.012	0.199	11.621, 12.403	-1.771	0.049	-1.868, -1.675
Distance from road (km)	-0.833	0.054	-0.939, -0.728	-1.532	0.011	-1.554, -1.511
Distance from houses (km)	-0.819	0.023	-0.864, -0.773	-0.239	0.006	-0.249, -0.228
Elevation (100 MSL)	0.664	0.027	0.610, 0.718	-0.297	0.003	-0.303, -0.297
Slope (degrees)	-0.021	0.002	-0.024, -0.018	-0.034	0.001	-0.036, -0.031

349

350 Between August 2013 and December 2015, 4814 *An. balabacensis* were caught from 328 sampling
351 nights in 155 unique locations. The median biting rate was 2.1 bites per night per person, ranging
352 from 0 – 28 bites per person per night (Figure 4). Despite monthly variation, no significant time lags
353 or seasonal patterns in mosquito biting rates were identified (Table 4). Although no associations
354 were identified between land classification and vector density in this site, models identified positive
355 relationships with enhanced vegetation indices (EVI) and negative associations with distance to
356 forest and human population density (Table 5). Of 1524 mosquitoes tested for *Plasmodium*
357 sporozoites, the median sporozoite rate was 0.24% (95% CI: 0.09 – 0.58%).

358

359 **Table 4.** Model selection statistics for mosquito biting rates

Model		DIC*	Marginal Likelihood	Model complexity*	RMSE*	Mean log-score (CPO)
M1	No spatial or temporal effect	2367.03	-1196.61	4.12	4.99	3.61
M2	Spatial effect only	2292.97	-1175.47	40.03	4.42	4.16
M3	Spatial effect + month as	2282.88	-1173.68	43.99	4.24	3.90

	fixed effect					
M4	Spatial effect + month as random effect	2222.89	-1155.91	50.28	4.05	3.61
M5	Spatial effect + month as random walk	2225.43	-1167.79	47.55	4.09	3.63

Table 5. Posterior rate ratio estimates and 95% Bayesian credible interval (BCI) for model 4 of mosquito biting rates

Covariate	95% BCI Rate Ratio		
	Mean	2.5%	97.5%
Population density	0.963	0.916	1.004
EVI	3.185	1.185	8.532
Distance to forest (100m)	0.926	0.871	0.976
Spatial range (km)	3.120	0.514	6.926

Figure 4. Mosquito biting rates. A. *An. balabacensis* biting rate per person-night from data collected in Matunggong, B. Predicted mean *An. balabacensis* biting rates per month from spatiotemporal models, C. Predicted number of bites for all individuals residing in Matunggong by distance from secondary forest, and by D. Distance from households

For individuals included in the GPS tracking study in Matunggong, where both human movement and entomology data was available, we calculated exposure risks as a derived quantity from utilisation distributions and mosquito biting rate models. Exposure varied markedly between individuals, with an overall 150-fold difference in predicted mean probabilities of infected bites per night (range: 0.00005-0.0078) (Table 6). No clear differences were observed between genders, age groups or occupations of individuals sampled and there was no association between risk and distance travelled.

Table 6. Probabilities of infected bites per night for sampled individuals in Matunggong by demographic characteristics

	Predicted infectious bites per night (median (IQR))
Demographic group	
Men	0.00157 (0.000804, 0.00289)
Women	0.00219 (0.000864, 0.00307)
Children (under 15)	0.00131 (0.000812, 0.00330)
Occupation	
Farming	0.00180 (0.00101, 0.00362)
Plantation work	0.00216 (0.000680, 0.00278)
Student	0.00143 (0.000915, 0.00304)
Other	0.00225 (0.000852, 0.00302)
No employment/ housewife	0.00142 (0.000297, 0.00263)

Using the resource utilisation function with demographic and spatial data for all individuals in Matunggong, we predicted community-wide space use and estimated exposure to infected mosquitoes (Figure 5). The predicted number of person nights per grid cell for the entire community ranged from 0 to 12.79 (median: 0.01, IQR: 0.0004 – 0.99), with the mean probability of a community member exposed to an infected bite per grid cell of 0.00082 (IQR: 0.00001, 0.00050). Although over 43% of the study site is forest and relatively high biting rates were predicted in forests during the study period (mean: 1.94, range: 0.04 – 12.59), this habitat was rarely used by people in the evenings, with less than 8% of predicted person-nights in forests. Models only based on mosquito biting rates and not including human space use predicted 42% of infectious bites occurred in forested areas and only 8.6% of bites occurring within 100m of houses (Figure 5C). In contrast, when space use patterns are included, over 91% of predicted infected bites were predicted within 500m of houses (Figure 5D). Highest exposure risks were consistently found near forest edges and in close proximity to households, despite spatial and temporal heterogeneity and model uncertainty (Figure 4).

Figure 5. A. Land use in Matunggong site, B. Predicted number of person- nights for entire community per grid cell, C. Predicted mosquito biting rates, D. Predicted infected bites per grid cell

Discussion

This study highlights the importance of human space use in different land cover types in determining exposure to zoonotic and vector-borne diseases such as *P. knowlesi*. Although *P. knowlesi* has previously been associated with forest exposure (e.g. (19)) and higher biting rates have been reported in forest interiors (23), this novel approach incorporating both mosquito and human space use data provides a new perspective on peri-domestic transmission, with more than 90% of infectious bites predicted in areas surrounding households at forest edges. This study additionally demonstrates the utility of ecological methods to understand human movement and identify geographical areas associated with higher contact with disease vectors.

Within these communities, local movement patterns during peak vector times were largely predictable and could be explained by spatial and environmental factors. However, despite this finding, there was substantial variation in predicted exposure between individuals as a result of heterogeneity in habitats used. No significant differences in exposure were predicted between men and women, with individuals with high exposure risks identified across occupational and age groups. Although this finding differs from clinical reports, a comprehensive survey within this community identified equal proportions of men and women exposed to *P. knowlesi* as evidenced by specific antibody responses and data on asymptomatic infections suggests higher numbers of non-clinical infections in women (30, 42). While infrequent events or long-range movements (such as hunting trips) may contribute to these differences in clinical cases and may not have been captured within

424 this two-week sampling period within the study site, this analysis highlights the importance of
425 routine movements into local environments in shaping exposure risks.
426
427 This improved understanding of how local human land use is related to exposure risk has important
428 implications for surveillance and control programmes. Malaria control programmes often rely on
429 interventions within the house, such as insecticide treated bednets and indoor residual spraying;
430 however, movements outside during peak biting times illustrate the importance of also targeting
431 outdoor transmission. The identification of areas where exposure is likely to occur can further be
432 used to refine interventions; for example, although insecticide treated hammocks have been
433 proposed for deep forest environments, larval source management may be more appropriate to
434 target environments in close proximity to houses. Although initial *P. knowlesi* cases were primarily
435 identified in adult men living and working in forests (20), this study illustrates the potential
436 importance of peri-domestic habitats in transmission and provides quantitative insight on mixing
437 between people and infected mosquitoes in forest fringe areas. As Malaysia moves towards malaria
438 elimination, surveillance systems are incorporating novel focal investigation methods, including
439 monitoring changes in local land use and populations at risk (43). In additional to routine vector
440 surveillance, this study highlights the need to incorporate measures of human space when defining
441 risk zones.
442
443 Even with the large and highly detailed movement dataset analysed, this study was limited by the
444 availability of mosquito data; as human landing catch data were assembled from other studies, there
445 was not uniform spatial and temporal coverage of the study site increasing uncertainty. The limited
446 mosquito data availability precluded development of mosquito biting rate models for Limbuak and
447 other outlying islands. An additional limitation to estimating mosquito biting rates was the difficulty
448 obtaining spatially and temporally resolute remote sensing data for predictors due to high cloud
449 cover (44). As few positive mosquitoes were identified, uniform estimates of sporozoite rates based

on available data were used across the Matunggong site; if further data was available, these models could be refined to incorporate estimates of human and macaque density, mosquito biting preferences in different habitats and infection levels in all hosts (45). Additionally, as this study was designed to quantitatively estimate time spent in different landscapes, further studies could explore other aspects of land use, such as the purposes of travel, activities undertaken or practices used to modify or management land cover.

Despite these limitations, this is the first large-scale study to utilise GPS tracking data and ecological methods to create fine-scale maps of exposure risk. This study highlights the importance of incorporating heterogenous patterns of human space use into disease models, as the majority of human exposure may occur in areas with lower vector biting rates but greater probabilities of human use. Further, results quantitatively illustrate the importance of forest edges and local habitat in *P. knowlesi* transmission and can inform understanding of other zoonotic and vector-borne diseases.

Acknowledgements

We would like to thank the MONKEYBAR project team and the participants in Sabah, Malaysia for their help with these studies. We acknowledge the Medical Research Council, Natural Environmental Research Council, Economic and Social Research Council and Biotechnology and Biosciences Research Council for funding received for this project through the Environmental and Social Ecology of Human Infectious Diseases Initiative, grant no. G1100796. This work was additionally supported by the National Socio-Environmental Synthesis Center (SESYNC).

472 **References:**

473 1. Lambin EF, Tran A, Vanwambeke SO, Linard C, Soti V. Pathogenic landscapes: interactions
474 between land, people, disease vectors, and their animal hosts. Int J Health Geogr. 2010;9:54.
475 2. Patz JA, Daszak P, Tabor GM, Aguirre AA, Pearl M, Epstein J, et al. Unhealthy landscapes:
476 Policy recommendations on land use change and infectious disease emergence. Environ Health
477 Perspect. 2004;112(10):1092-8.
478 3. Stoddard ST, Forshey BM, Morrison AC, Paz-Soldan VA, Vazquez-Prokopec GM, Astete H, et
479 al. House-to-house human movement drives dengue virus transmission. Proc Natl Acad Sci U S A.
480 2013;110(3):994-9.
481 4. Stoddard ST, Morrison AC, Vazquez-Prokopec GM, Paz Soldan V, Kochel TJ, Kitron U, et al.
482 The role of human movement in the transmission of vector-borne pathogens. PLoS Negl Trop Dis.
483 2009;3(7):e481.
484 5. Pindolia DK, Garcia AJ, Wesolowski A, Smith DL, Buckee CO, Noor AM, et al. Human
485 movement data for malaria control and elimination strategic planning. Malar J. 2012;11(205).
486 6. Moyes CL, Shearer FM, Huang Z, Wiebe A, Gibson HS, Nijman V, et al. Predicting the
487 geographical distributions of the macaque hosts and mosquito vectors of Plasmodium knowlesi
488 malaria in forested and non-forested areas. Parasit Vectors. 2016;9(1):242.
489 7. Imai N, White MT, Ghani AC, Drakeley CJ. Transmission and control of Plasmodium knowlesi:
490 a mathematical modelling study. PLoS Negl Trop Dis. 2014;8(7):e2978.
491 8. Fornace KM, Abidin TR, Alexander N, Brock P, Grigg MJ, Murphy A, et al. Association
492 between Landscape Factors and Spatial Patterns of Plasmodium knowlesi Infections in Sabah,
493 Malaysia. Emerg Infect Dis. 2016;22(2):201-8.
494 9. Shearer FM, Huang Z, Weiss DJ, Wiebe A, Gibson HS, Battle KE, et al. Estimating
495 Geographical Variation in the Risk of Zoonotic Plasmodium knowlesi Infection in Countries
496 Eliminating Malaria. PLoS Negl Trop Dis. 2016;10(8):e0004915.
497 10. Brock PM, Fornace KM, Grigg MJ, Anstey NM, William T, Cox J, et al. Predictive analysis
498 across spatial scales links zoonotic malaria to deforestation. Proceedings of the Royal Society B.
499 2019;286(1894).
500 11. IPCC. Land use, land-use change, and forestry. Watson RT, Noble IR, Bolin B, Ravindranath
501 NH, Verado DJ, Dokken DJ, editors. UK: Cambridge University Press; 2000.
502 12. Acevedo MA, Prosper O, Lopiano K, Ruktanonchai N, Caughlin TT, Martcheva M, et al. Spatial
503 heterogeneity, host movement and mosquito-borne disease transmission. PLoS One.
504 2015;10(6):e0127552.
505 13. Yakob L, Lloyd AL, Kao RR, Ferguson HM, Brock PM, Drakeley C, et al. Plasmodium knowlesi
506 invasion following spread by infected mosquitoes, macaques and humans. Parasitology.
507 2018;145(1):101-10.
508 14. Chang HH, Wesolowski A, Sinha I, Jacob CG, Mahmud A, Uddin D, et al. Mapping imported
509 malaria in Bangladesh using parasite genetic and human mobility data. Elife. 2019;8.
510 15. Wesolowski A, Qureshi T, Boni MF, Sundsoy PR, Johansson MA, Rasheed SB, et al. Impact of
511 human mobility on the emergence of dengue epidemics in Pakistan. Proc Natl Acad Sci U S A.
512 2015;112(38):11887-92.
513 16. Wesolowski A, Metcalf CJ, Eagle N, Kombich J, Grenfell BT, Bjornstad ON, et al. Quantifying
514 seasonal population fluxes driving rubella transmission dynamics using mobile phone data. Proc Natl
515 Acad Sci U S A. 2015;112(35):11114-9.
516 17. Wesolowski A, Buckee CO, Engo-Monsen K, Metcalf CJE. Connecting Mobility to Infectious
517 Diseases: The Promise and Limits of Mobile Phone Data. J Infect Dis. 2016;214(suppl_4):S414-S20.
518 18. Vazquez-Prokopec GM, Bisanzio D, Stoddard ST, Paz-Soldan V, Morrison AC, Elder JP, et al.
519 Using GPS technology to quantify human mobility, dynamic contacts and infectious disease dynamics
520 in a resource-poor urban environment. PLoS One. 2013;8(4):e58802.

521 19. Grigg MJ, Cox J, William T, Jelip J, Fornace KM, Brock PM, et al. Individual-level factors
522 associated with the risk of acquiring human Plasmodium knowlesi malaria in Malaysia: a case control
523 study. Lancet Planetary Health. 2017;1:e97-104.
524 20. Singh B, Kim Sung L, Matusop A, Radhakrishnan A, Shamsul SS, Cox-Singh J, et al. A large
525 focus of naturally acquired Plasmodium knowlesi infections in human beings. Lancet.
526 2004;363(9414):1017-24.
527 21. Yasuoka J, Levins R. Impact of deforestation and agricultural development on anopheline
528 ecology and malaria epidemiology. Am J Trop Med Hyg. 2007;76(3):450-60.
529 22. Barber BE, William T, Dhararaj P, Anderios F, Grigg MJ, Yeo TW, et al. Epidemiology of
530 Plasmodium knowlesi malaria in north-east Sabah, Malaysia: family clusters and wide age
531 distribution. Malar J. 2012;11:401.
532 23. Wong ML, Chua TH, Leong CS, Khaw LT, Fornace K, Wan-Sulaiman WY, et al. Seasonal and
533 Spatial Dynamics of the Primary Vector of Plasmodium knowlesi within a Major Transmission Focus
534 in Sabah, Malaysia. PLoS Negl Trop Dis. 2015;9(10):e0004135.
535 24. Manin BO, Ferguson HM, Vythilingam I, Fornace K, William T, Torr SJ, et al. Investigating the
536 Contribution of Peri-domestic Transmission to Risk of Zoonotic Malaria Infection in Humans. PLoS
537 Negl Trop Dis. 2016;10(10):e0005064.
538 25. Lee KS, Divis PC, Zakaria SK, Matusop A, Julin RA, Conway DJ, et al. Plasmodium knowlesi:
539 reservoir hosts and tracking the emergence in humans and macaques. PLoS Pathog.
540 2011;7(4):e1002015.
541 26. Chua TH, Manin BO, Daim S, Vythilingam I, Drakeley C. Phylogenetic analysis of simian
542 Plasmodium spp. infecting Anopheles balabacensis Baisas in Sabah, Malaysia. PLoS Negl Trop Dis.
543 2017;11(10):e0005991.
544 27. Hartemink N, Vanwambeke SO, Purse BV, Gilbert M, Van Dyck H. Towards a resource-based
545 habitat approach for spatial modelling of vector-borne disease risks. Biol Rev Camb Philos Soc.
546 2015;90(4):1151-62.
547 28. Papworth SK, Bunnefeld N, Slocombe K, Milner-Gulland EJ. Movement ecology of human
548 resource users: using net squared displacement, biased random bridges and resource utilization
549 functions to quantify hunter and gatherer behaviour. Methods in Ecology and Evolution.
550 2012;3(3):584-94.
551 29. Benhamou S. Dynamic approach to space and habitat use based on biased random bridges.
552 PLoS One. 2011;6(1):e14592.
553 30. Fornace KM, Herman LS, Abidin TR, Chua TH, Daim S, Lorenzo PJ, et al. Exposure and
554 infection to Plasmodium knowlesi in case study communities in Northern Sabah, Malaysia and
555 Palawan, The Philippines. PLoS Negl Trop Dis. 2018;12(6):e0006432.
556 31. DAAC NL. MODIS/ Terra Vegetation Indices 16-Day L3 Global 250m Grid SIN V006. Sioux
557 Falls, South Dakota: USGS Earth Resources Observation and Science (EROS) Center.
558 32. Johnston R, Brady HE. The rolling cross-section design. Electoral Studies. 2002;21(2):283-95.
559 33. Hooten MB, Hanks EM, Johnson DS, Alldredge MW. Reconciling resource utilization and
560 resource selection functions. J Anim Ecol. 2013;82(6):1146-54.
561 34. Blangiardo M, Cameletti M. Spatial and Spatio-temporal Bayesian Models with R-INLA.
562 Chichester, United Kingdom: John Wiley & Sons, Ltd; 2015.
563 35. Sadykova D, Scott BE, De Dominicis M, Wakelin SL, Sadykov A, Wolf J. Bayesian joint models
564 with INLA exploring marine mobile predator-prey and competitor species habitat overlap. Ecol Evol.
565 2017;7:5212-26.
566 36. Barbet-Massin M, Jiguet F, Albert CH, Thuiller W. Selecting pseudo-absences for species
567 distribution models: how, where and how many? Methods in Ecology and Evolution. 2012;3:327-38.
568 37. Rue H, Martino S, Chopin N. Approximate Bayesian inference for latent Gaussian models by
569 using integrated nested Laplace approximations. Journal of the Royal Statistical Society.
570 2009;71(Part 2):319-92.

571 38. Ng SH, Homathevi R, Chua TH. Mosquitoes of Kudat: species composition and their medical
572 importance (Diptera: Culicidae). Serangga. 2016;21(2):149-62.
573 39. Lindgren F, Rue H. Bayesian Spatial Modelling with R-INLA. Journal of Statistical Software.
574 2015;63(19).
575 40. Lindgren F, Rue H, Lindstrom J. An explicit link between Gaussian fields and Gaussian Markov
576 random fields: the stochastic partial differential equation approach. Statistical Methodology.
577 2011;73(4):423-98.
578 41. Held L, Schrodle B, Rue H. Posterior and Cross-validatory Predictive Checks: A Comparison of
579 MCMC and INLA. In: Kneib T, Tutz G, editors. Statistical Modelling and Regression Structures:
580 Physica-Verlag HD; 2010.
581 42. Fornace KM, Nuin NA, Betson M, Grigg MJ, William T, Anstey NM, et al. Asymptomatic and
582 Submicroscopic Carriage of Plasmodium knowlesi Malaria in Household and Community Members of
583 Clinical Cases in Sabah, Malaysia. J Infect Dis. 2015.
584 43. Sektor Penyakit Bawaan Vektor Bahagian Kawalan Penyakit Kementarian Kesihatan
585 Malaysia. Garis Panduan Pencegahan Malaria Re-Introduction di Malaysia. Putra Jaya: Kementerian
586 Kesihatan Malaysia; 2016. Contract No.: KKM/TM/620/2016.
587 44. Weiss DJ, Mappin B, Dalrymple U, Bhatt S, Cameron E, Hay SI, et al. Re-examining
588 environmental correlates of Plasmodium falciparum malaria endemicity: a data-intensive variable
589 selection approach. Malar J. 2015;14:68.
590 45. Yakob L, Bonsall MB, Yan G. Modelling knowlesi malaria transmission in humans: vector
591 preference and host competence. Malar J. 2010;9:329.

592

593

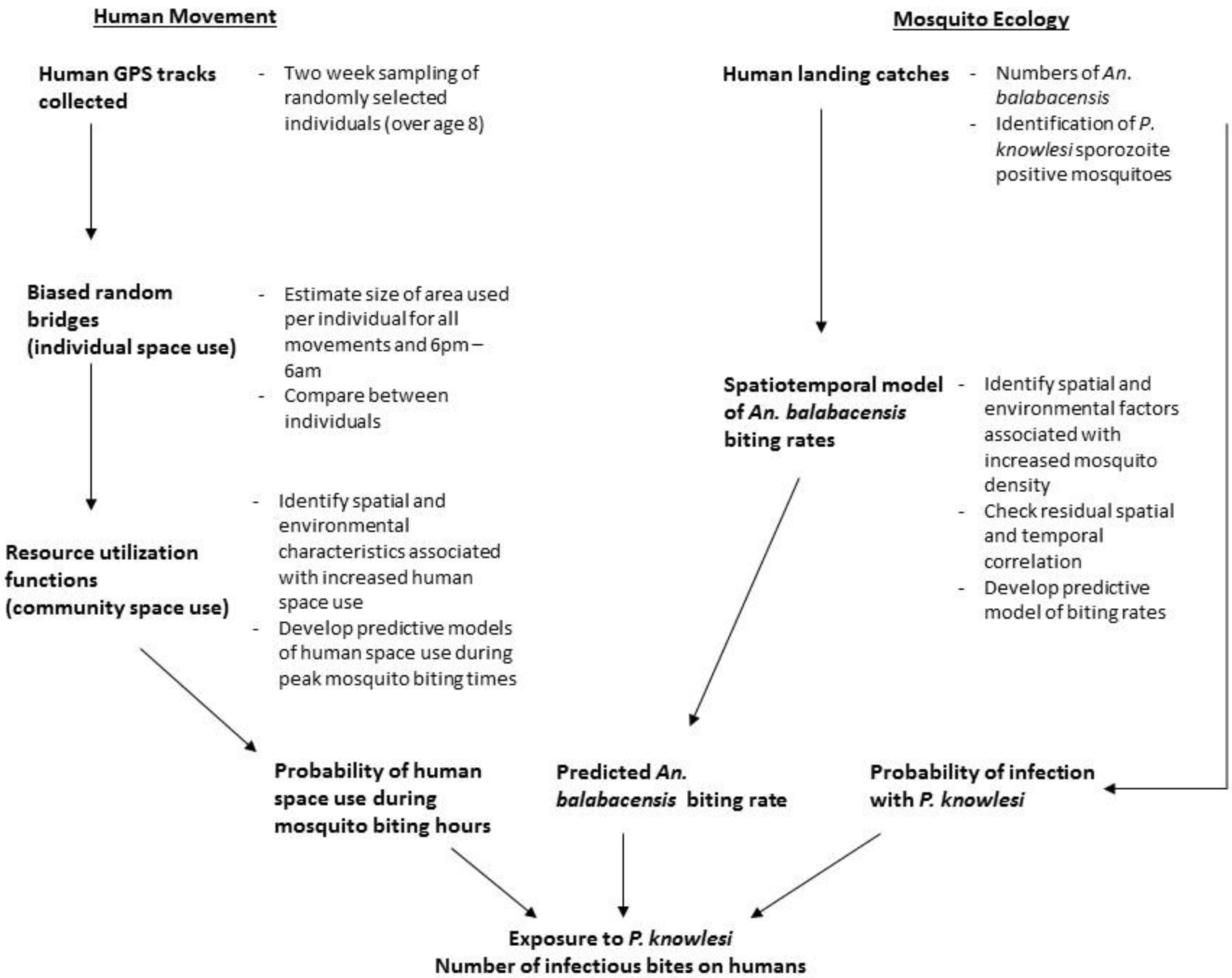
Human Movement
Mosquito Ecology
Human GPS tracks collected
- Two week sampling of randomly selected individuals (over age 8)
Human landing catches
- Numbers of An. balabacensis
- Identification of P. knowlesi sporozoite positive mosquitoes
Biased random bridges (individual space use)
- Estimate size of area used per individual for all movements and 6pm – 6am
- Compare between individuals
Spatiotemporal model of An. balabacensis biting rates
- Identify spatial and environmental factors associated with increased mosquito density
- Check residual spatial and temporal correlation
- Develop predictive model of biting rates
Resource utilization functions (community space use)
- Identify spatial and environmental characteristics associated with increased human space use
- Develop predictive models of human space use during peak mosquito biting times
Probability of human space use during mosquito biting hours
Predicted An. balabacensis biting rate
Probability of infection with P. knowlesi
Exposure to P. knowlesi
Number of infectious bites on humans

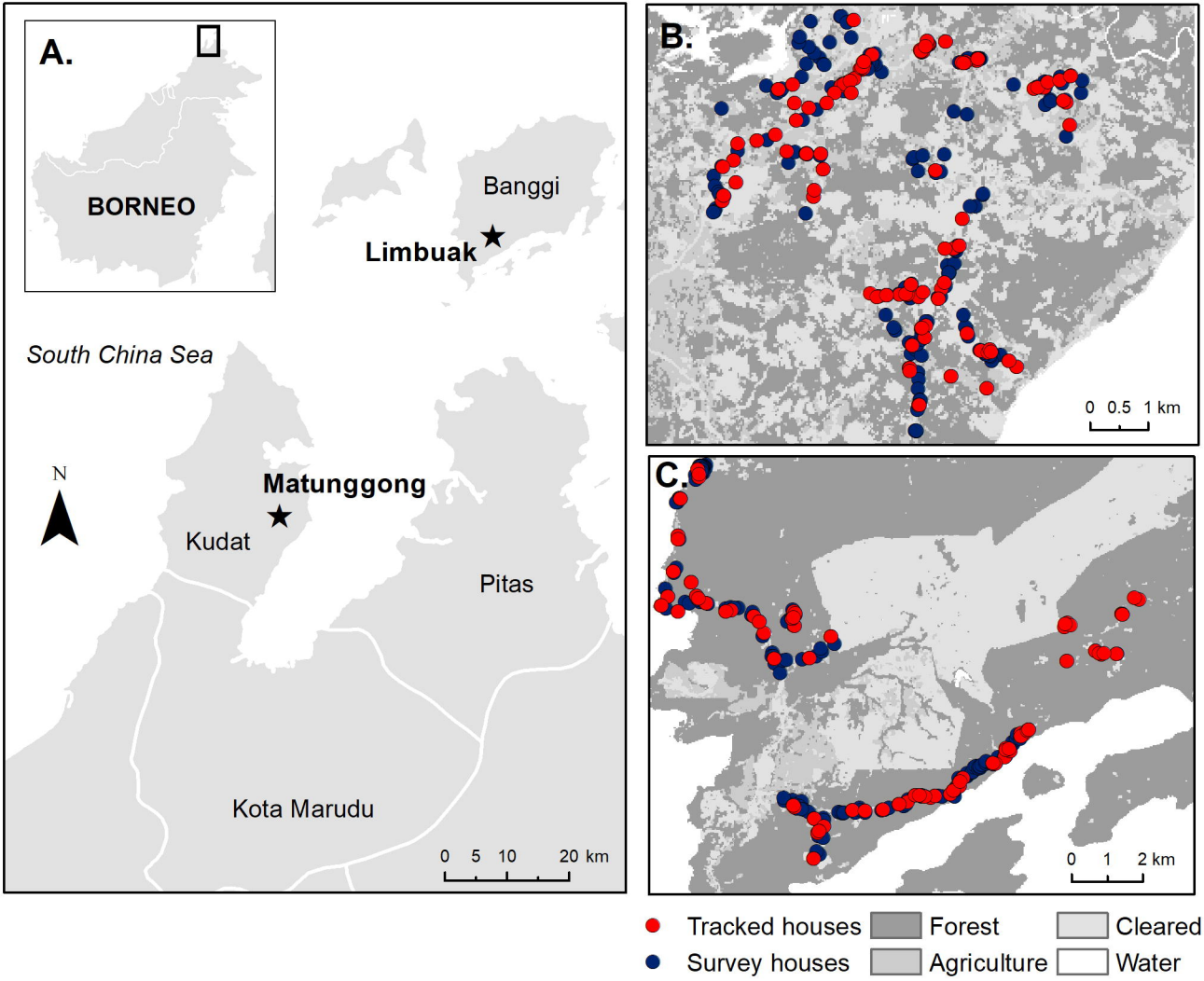
A.
BORNEO
Banggi
Limbuak
South China Sea
N
Matunggong
Kudat
Pitas
Kota Marudu
0 5 10 20 km
B.
0 0.5 1 km
C.
0 1 2 km
Tracked houses
Survey houses
Forest
Agriculture
Cleared
Water

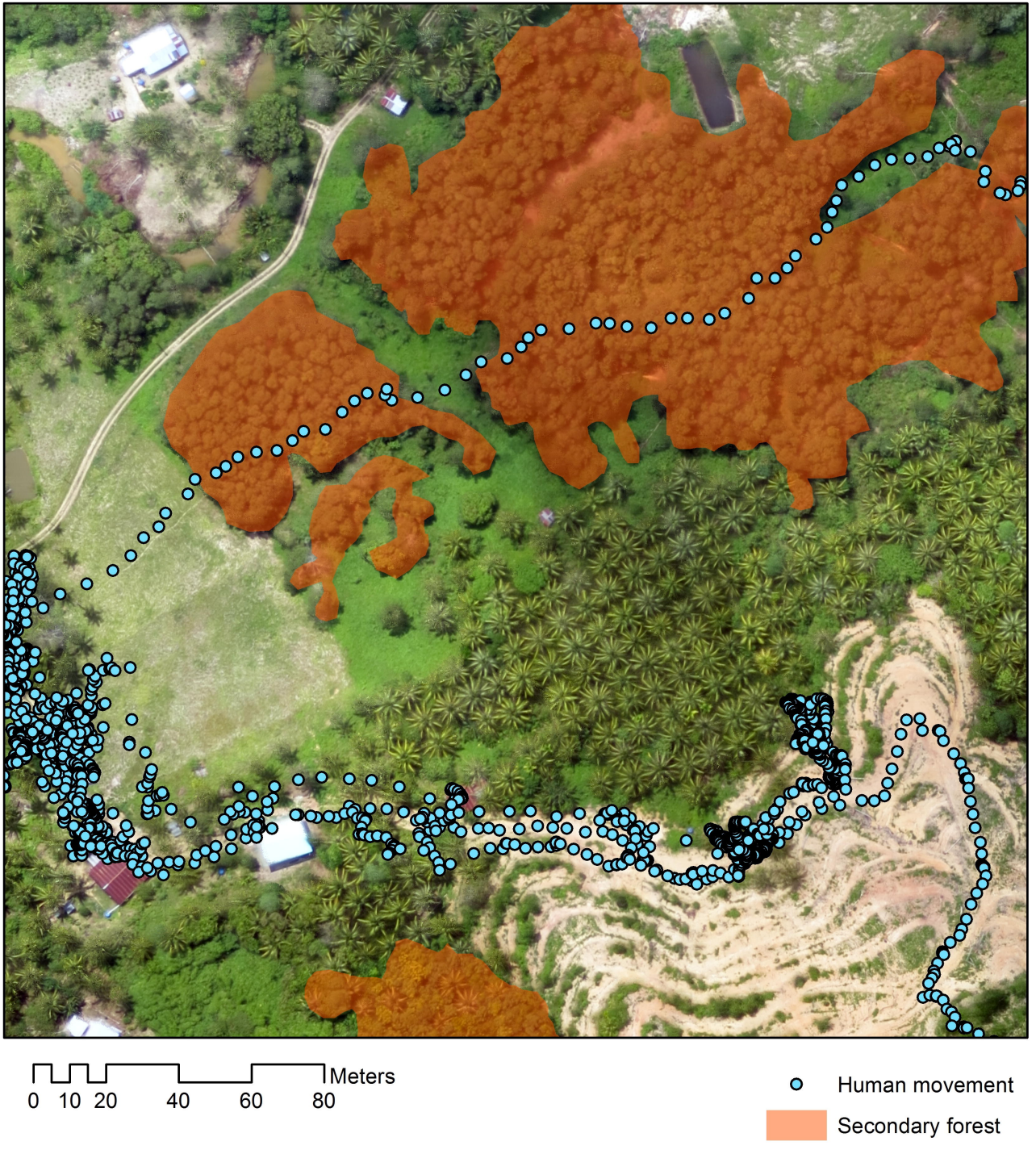
Meters
0
10
20
40
60
80
Human movement
Secondary forest

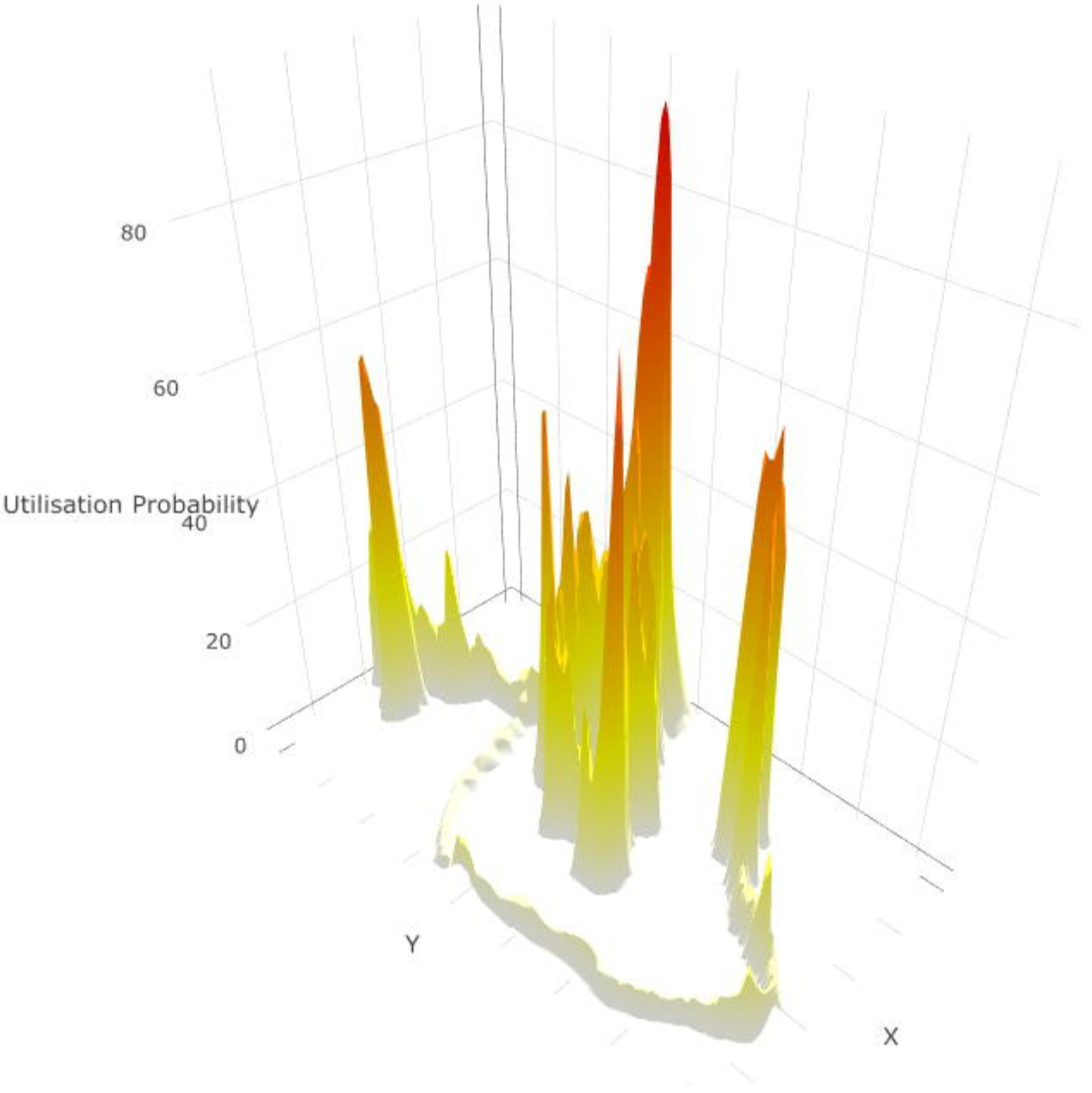
80
60
Utilisation Probability
40
20
0
Y
X

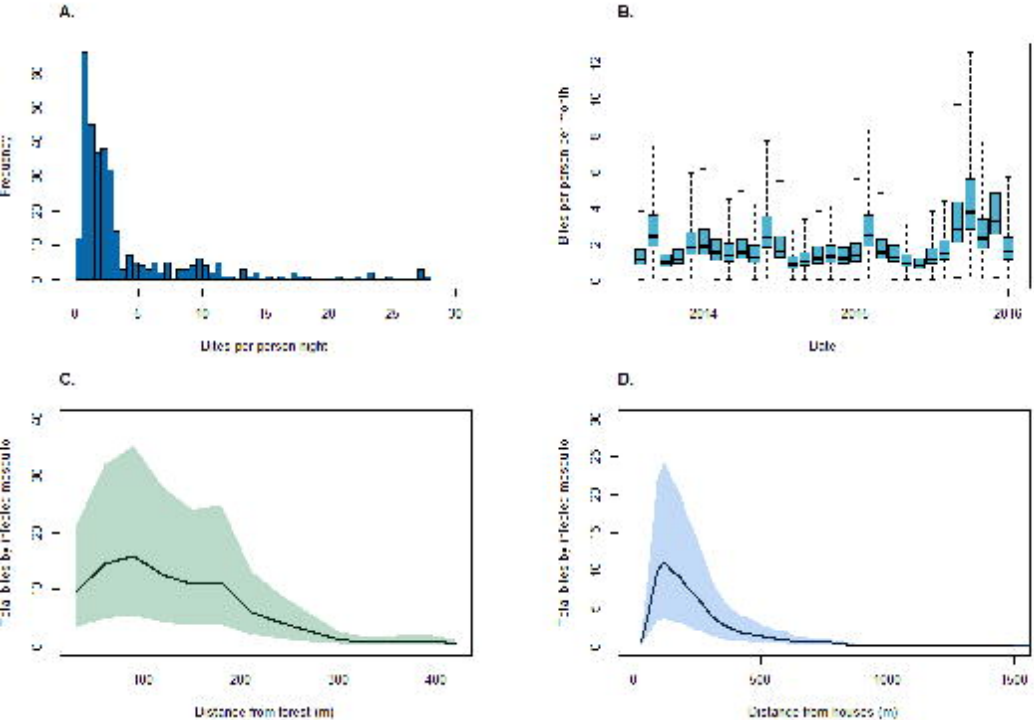
A.
Bites per person night
B.
Bites per person per month
Date
C.
Distance from forest (m)
D.
Distance from houses (m)

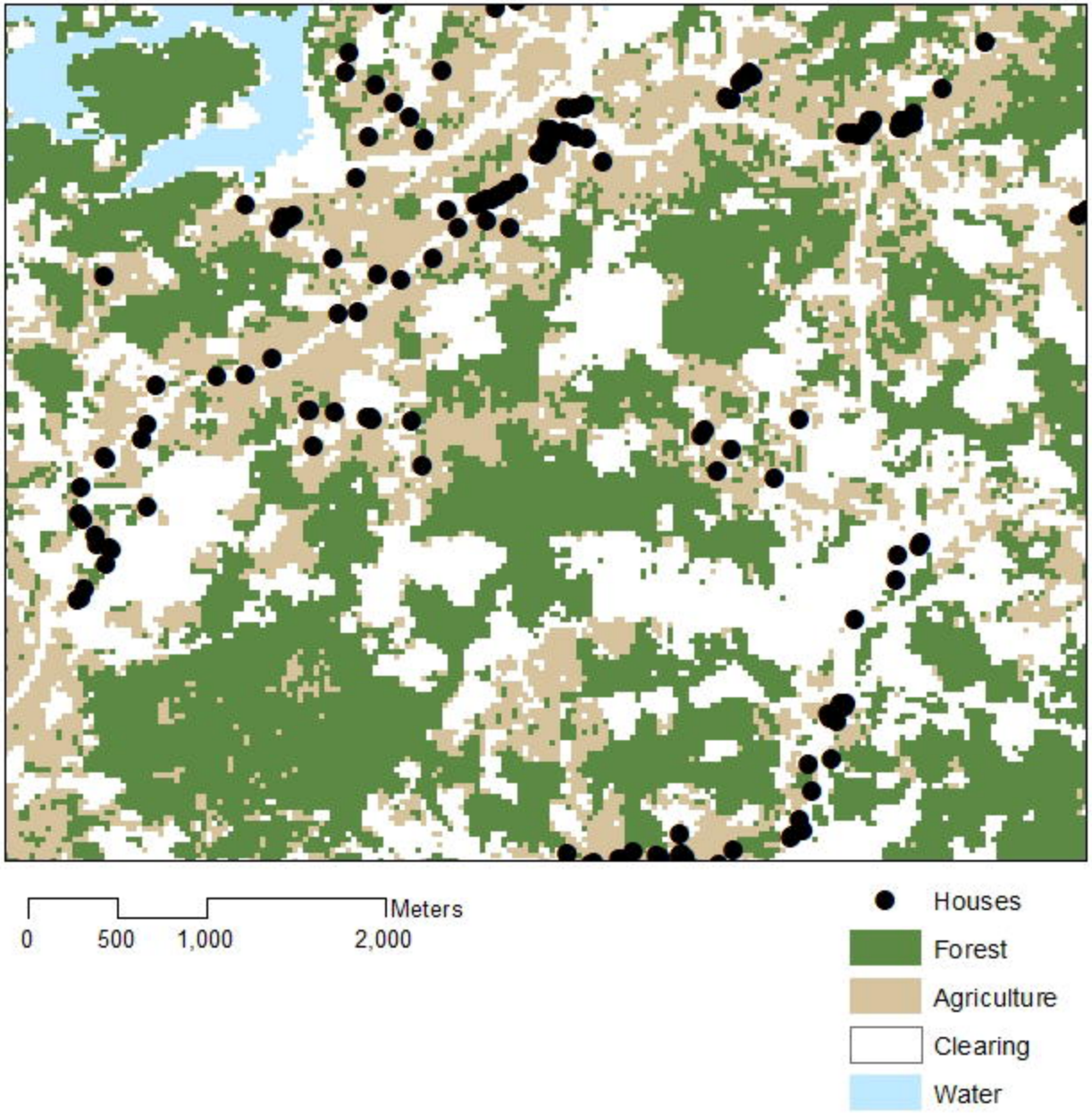
Meters
0
500
1,000
2,000
Houses
Forest
Agriculture
Clearing
Water

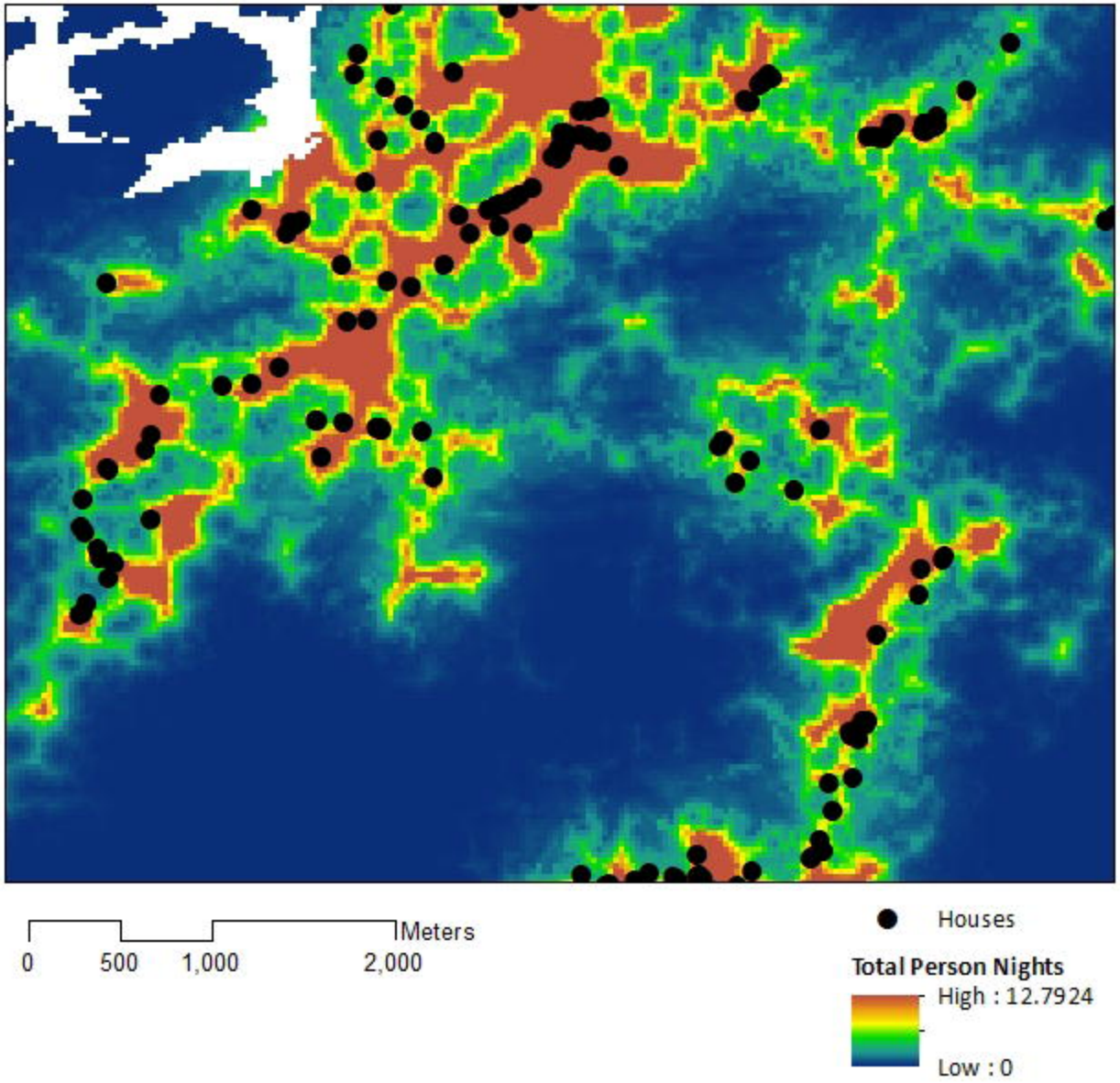
0
500
1,000
2,000
Meters
Houses
Total Person Nights
High : 12.7924
Low : 0

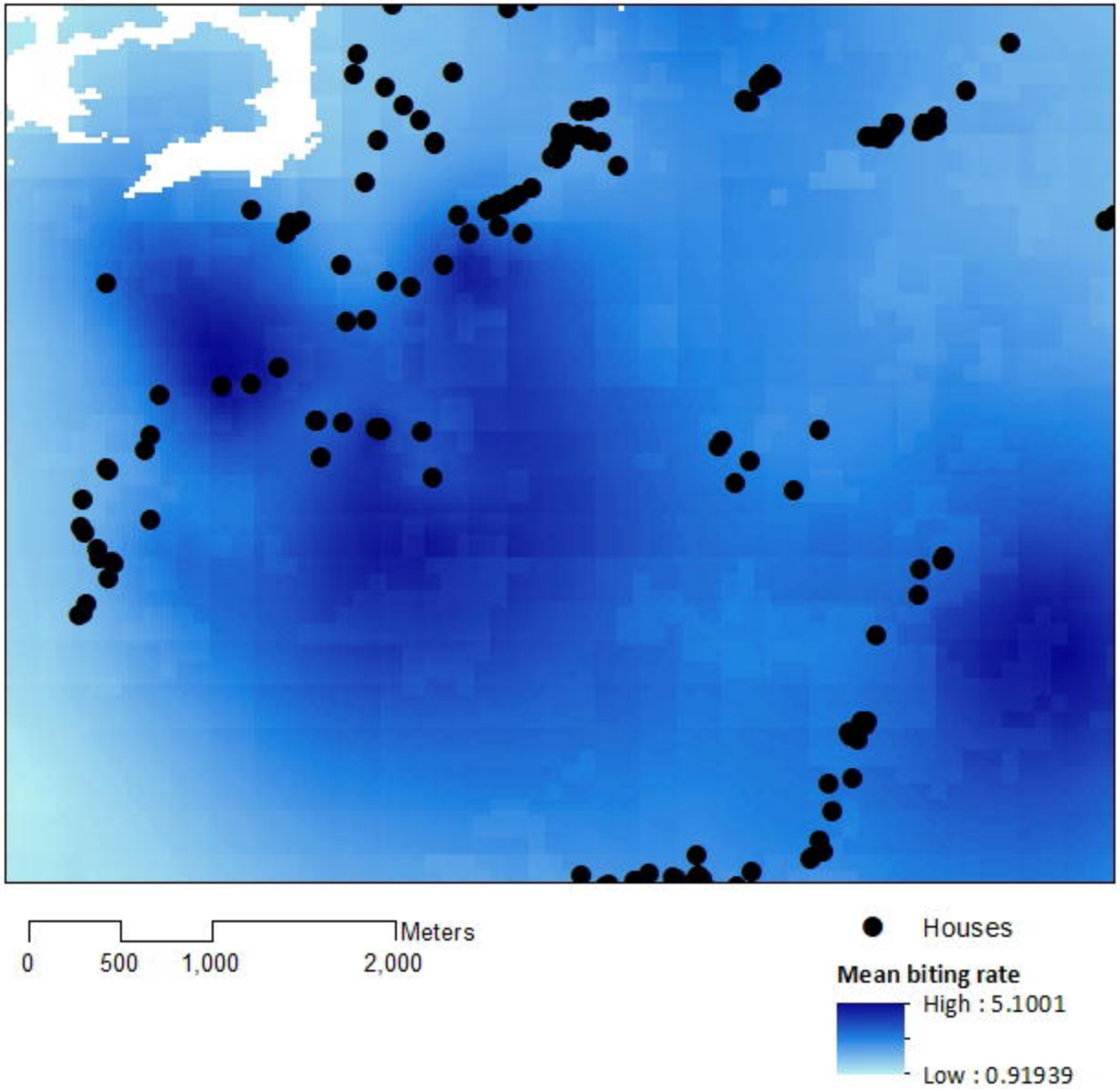
Meters
0
500
1,000
2,000
Houses
Mean biting rate
High : 5.1001
Low : 0.91939

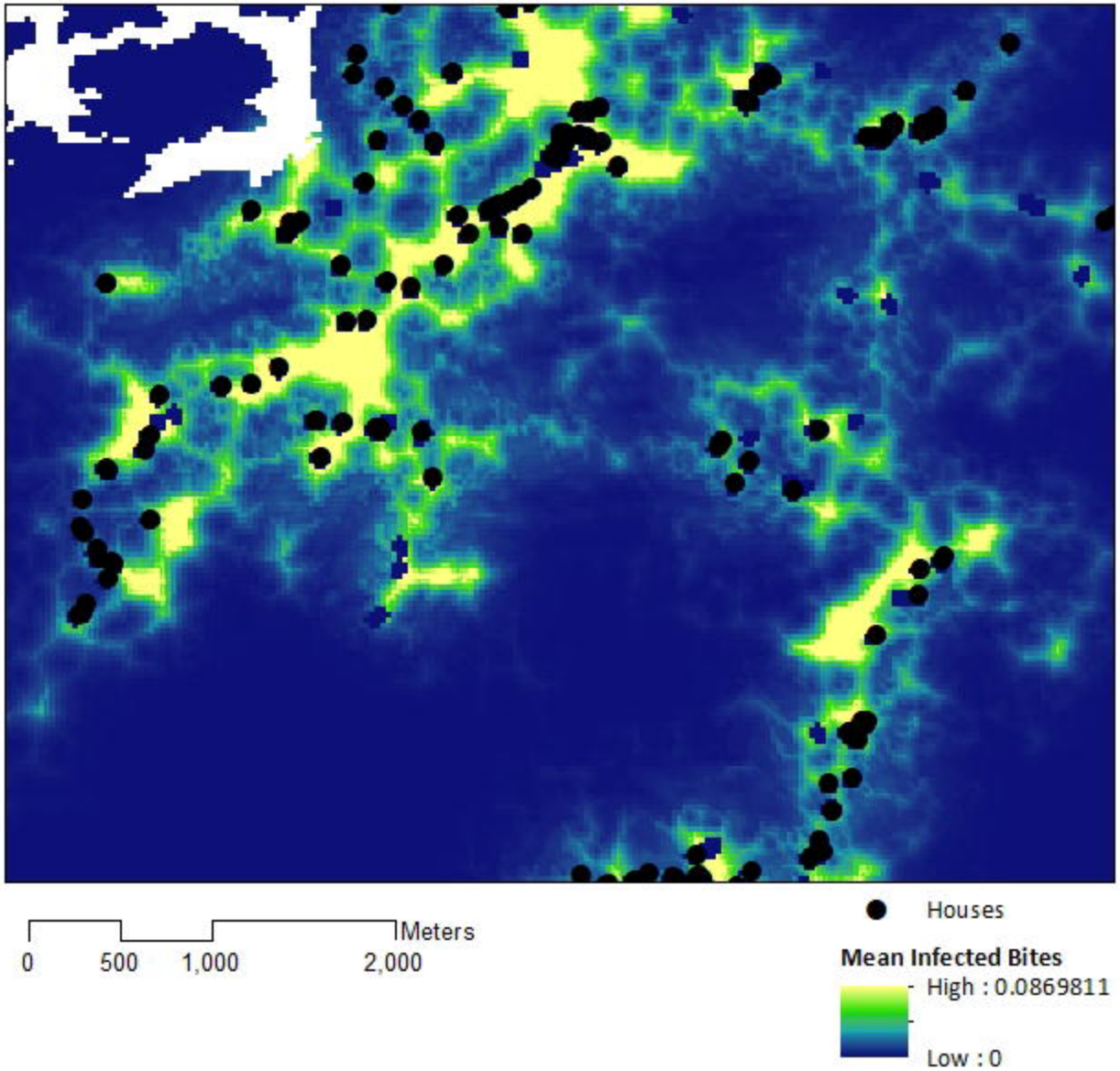
Meters
0
500
1,000
2,000
Houses
Mean Infected Bites
High : 0.0869811
Low : 0